PROCEEDINGS OF SCIENCE

Acoustic signatures of ultra-high-energy neutrinos

Felix Henningsen[a,*] **and Juan Ammeram-Yebra**[b]

[a] *Simon Fraser University*
Department of Physics, Burnaby, Canada V5A 1S6
[b] *Instituto Galego de Física de Altas Enerxías (IGFAE)*
Universidade de Santiago de Compostela, 15782 Santiago de Compostela, Spain

E-mail: felix_henningsen@sfu.ca, juan.ammerman.yebra@usc.es

Detecting ultra-high-energy neutrinos has been a long-standing goal of astroparticle physics at the energy frontier. Radio and acoustic detection techniques have been investigated, with radio being the prevalent strategy for the last decade or two. The acoustic detection of neutrinos has faced significant challenges due to necessary array technologies, data filtering algorithms, and simulation tools. New technology and computing means, however, could be the foundation to re-open this window into the high-energy universe in the future. In this contribution, we present a first step in this direction, with preliminary work on simulating acoustic neutrino signatures with the CORSIKA 8 simulation framework.

10th International Workshop on Acoustic and Radio EeV Neutrino Detection Activities (ARENA2024)
11-14 June 2024
The Kavli Institute for Cosmological Physics, Chicago, IL, USA

*Speaker

PoS(ARENA2024)014

1. Introduction

The emerging field of ultra-high-energy particle astronomy is rapidly accelerating its efforts to detect the most energetic particles and their sources. Neutrinos are one of the key messenger particles for high-energy source identification and provide a potentially deep probe into cosmic accelerators [1–3]. For energies exceeding 10 PeV, detectors of many cubic-kilometer volumes are required to reach sensitivities for the low expected neutrino fluxes [4]. In addition, optical instrumentation for detecting neutrinos via the Cherenkov effect is difficult in such large volumes and not economical. Most recent experimental efforts thus target the detection of UHE neutrinos through radio emission [5–7] via the Askaryan effect [8]. The energy deposition of high-energy particle showers also generates acoustic waves [9–11] that can, in principle, be used to detect UHE neutrinos acoustically – see [12] for a review.

The knowledge about the resulting radio and acoustic pulse properties is critical for the simulation and estimation of detector properties. Previous works [13–15] have investigated the acoustic neutrino pulse formation in detail, but no state-of-the-art simulation framework is readily available for this purpose. In this contribution, we describe a novel simulation approach for the generation of acoustic neutrino signatures using the CORSIKA 8 simulation framework [16, 17].

2. Neutrino shower simulation

Neutrino showers at UHE energies can be simulated with CORSIKA 8 by default. For this work, however, our application had to be extended with neutrino interactions in water. The baseline simulation allows tracking of various shower observables, particle types, and total energy losses, but the acoustic pulse generation heavily depends on the total energy deposition and its profile profile in the medium. We thus developed a dedicated energy-loss tracker that continuously traces energy losses during shower development. This Radial Energy Deposition (RED) module tracks the energy deposition of the shower through all radial and longitudinal bins. The resulting profile then describes the energy deposition density of the shower. We then use these energy density profiles to generate Monte Carlo (MC) showers in three-dimensional space.. An example radial energy-loss profile and resulting MC shower projections in x-y and x-z are shown in fig. 1.

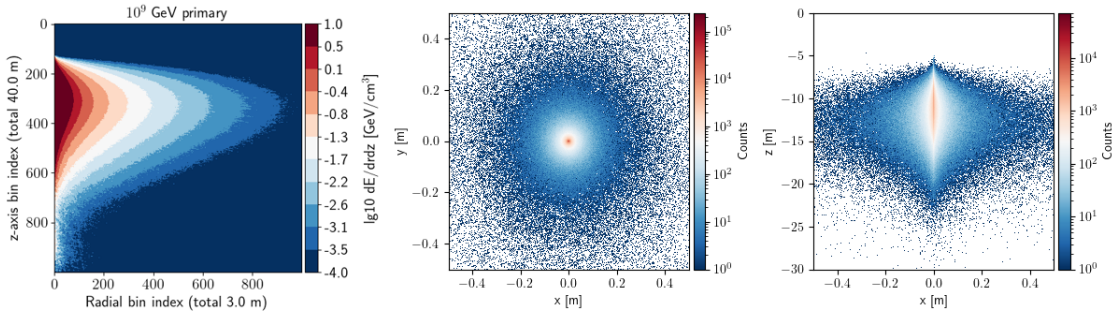

Figure 1: Example simulation of a 10^9 GeV ν_μ neutral-current neutrino shower in water with the radial energy deposition density (left) and the resulting three-dimensional shower profiles (center, right).

The MC showers are built by uniformly sampling the RED profile a finite number of times, thus adhering to the initial energy deposition but providing a discrete measure for the relative energy deposition per bin in three-dimensional space. This technique further saves valuable computation time and memory by tracing only two dimensions (radial and along the shower axis) during simulation.

3. Acoustic pulses

The energy deposition of the neutrino-induced shower leads to instantaneous water heating – or an explosion – that quickly relaxes to thermal equilibrium with the surrounding water body. This is governed by the thermo-acoustic effect [10, 11] and results in a time-dependent pressure variation $p'(\vec{r}, t)$ from the medium as described by the equation

$$\Delta p - \frac{1}{c_s^2}\frac{\partial^2 p}{\partial^2 t} = -\frac{\alpha}{C_p}\frac{\partial^2 q}{\partial t^2} \tag{1}$$

with volume expansion coefficient α, heat capacity C_p, speed of sound c_s, and energy deposition q. Thus, the characteristics of this pulse depend on the energy deposition, and the exact water properties at the interaction site. These acoustic pulses typically peak at frequencies below 20 kHz and can propagate through the water column for many kilometers [13].

To study the resulting pulses, we simulated a small set of neutrino interactions with primary energies of 10 PeV to 1 EeV. Each shower's RED profile was generated, and MC shower projections in three dimensions were derived. Then, as shown explicitly in [13], the velocity potential, $\Phi(t)$, of the shower for a given sensor location can be obtained by projecting the MC shower energy deposition onto a sensor at a defined position. The pressure pulse at the sensor location is then the time derivative of the velocity potential. This potential depends on the specific water properties as evident from eq. (1). For illustration, we use the Mediterranean Sea as described in [14] with $c_p = 3.8 \cdot 10^{-3}\,\mathrm{J\,kg^{-1}\,K^{-1}}$, $\alpha = 2 \cdot 10^{-4}\,\mathrm{K^{-1}}$ at 287 K, $c_s = 1542\,\mathrm{m\,s^{-1}}$ but no water attenuation or depth-dependent variation of speed of sound is considered. An example of the derived pressure pulse is shown in fig. 2.

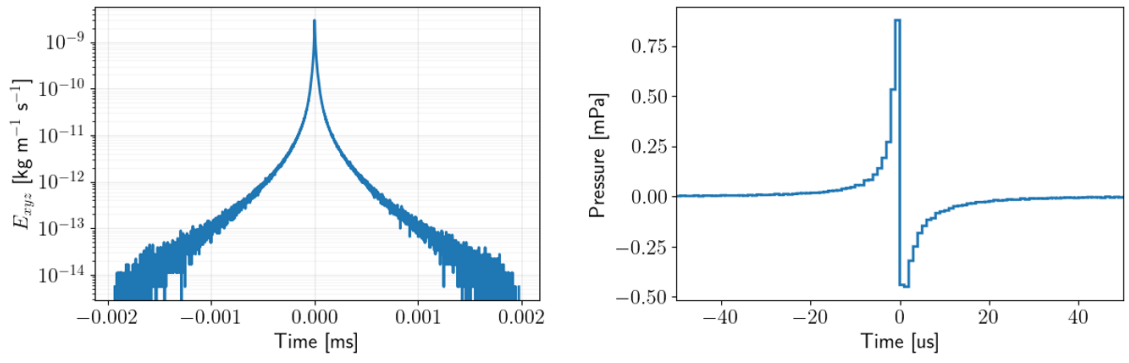

Figure 2: Velocity potential (left) and acoustic pressure pulse (right) for a 100 PeV muon neutrino primary in a neutral-current interaction based on CORSIKA 8 shower simulations. The water properties are assumed to resemble the Mediterranean Sea, with more details given in the text.

The acoustic signal's expected sharp angular distribution can be illustrated by placing the artificial pressure sensor at varying angles to the shower axis. As expected, fig. 3 confirms that the pressure amplitude drops sharply for angular deviations from the axis perpendicular to the maximum. This shape is commonly called the *acoustic pancake* and delivers an initial verification of this new simulation framework for acoustic pulses derived from neutrino interactions.

It should be noted that, in addition to water attenuation, the pressure pulse shape at different observation angles is heavily affected by the bending of acoustic rays in the water column due to speed of sound variation with depth. The eventual shape of the bipolar pulse at any relative sensor position thus needs to be carefully evaluated by ray-tracing the acoustic waves from the shower location to the sensor with the respective properties of the considered water column. This is not yet done here but will be added in the future.

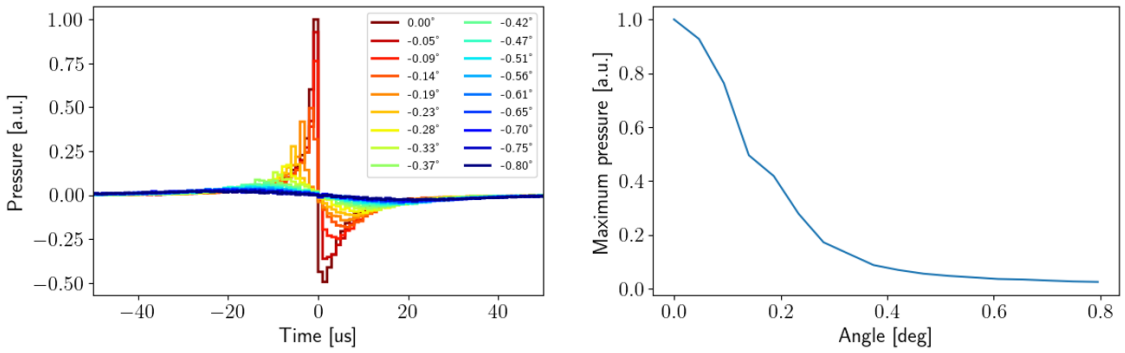

Figure 3: Angular distribution of the received pressure pulse relative to the shower axis for raw pulse waveforms (left) and the derived angular distribution (right). An angle of 0 degrees corresponds to the sensor placed perpendicular to the plane of maximum received pressure. No frequency-dependent water attenuation or acoustic ray-tracing has been applied.

Stochastic fluctuation of the pulse energy content, and thus the maximum pressure amplitude, is expected and results from the inelasticity distribution of the neutrino interaction. For neutrino energies of 10^8 – 10^{10} GeV, resulting acoustic pressure pulse amplitudes are in the range of 0.1 – 10 mPa at 1 km distance of the shower, however, without yet correcting for water attenuation. The order of magnitude of these pressure pulse amplitudes agrees well with previous simulation results [13, 14], and thus provides a preliminary baseline verification for our new, state-of-the-art simulation framework for the study of acoustic neutrinos at the highest energies.

4. Outlook

In this work, we report the successful implementation of ultra-high-energy neutrino interactions and resulting showers in water using the CORSIKA 8 simulation framework. This baseline is used to derive acoustic pulses for neutrino interactions with primary energies of 10^8 – 10^{10} GeV, which compare well in characteristics to those derived in previous works. We plan to further extend this framework by including acoustic ray propagation of the acoustic pressure pulse and the inclusion of arbitrary sensor arrays. This will enable feasibility and sensitivity studies of future acoustic detectors and their detection of ultra-high-energy neutrinos.

References

[1] The IceCube Collaboration, *Science* **2018**, *361*, (Eds.: M. Aartsen et al.), Publisher: American Association for the Advancement of Science, DOI 10.1126/science.aat1378.

[2] IceCube Collaboration et al., *Science* **2022**, *378*, Publisher: American Association for the Advancement of Science, 538–543.

[3] IceCube Collaboration, *Science* **2023**, *380*, Publisher: American Association for the Advancement of Science, 1338–1343.

[4] M. Ackermann et al., High-Energy and Ultra-High-Energy Neutrinos, arXiv:2203.08096 [astro-ph, physics:hep-ex, physics:hep-ph], **2022**.

[5] G. Collaboration et al., *Science China Physics Mechanics & Astronomy* **2020**, *63*, arXiv:1810.09994 [astro-ph, physics:hep-ex, physics:hep-ph], 219501.

[6] J. A. Aguilar et al., *Journal of Instrumentation* **2021**, *16*, arXiv:2010.12279 [astro-ph], P03025.

[7] S. Hallmann et al., Sensitivity studies for the IceCube-Gen2 radio array, arXiv:2107.08910 [astro-ph], **2021**.

[8] G. A. Askar'yan, *Sov. Phys. JETP* **1962**, *14*, 441–443.

[9] G. A. Askaryan, *The Soviet Journal of Atomic Energy* **1957**, *3*, 921–923.

[10] G. A. Askariyan et al., *Nuclear Instruments and Methods* **1979**, *164*, 267–278.

[11] J. G. Learned, *Physical Review D* **1979**, *19*, Publisher: American Physical Society, 3293–3307.

[12] R. Lahmann, *Nuclear and Particle Physics Proceedings*, 37th International Conference on High Energy Physics (ICHEP) **2016**, *273-275*, 406–413.

[13] S. Bevan et al., *Nuclear Instruments and Methods in Physics Research Section A: Accelerators Spectrometers Detectors and Associated Equipment* **2009**, *607*, arXiv:0903.0949 [astro-ph], 398–411.

[14] M. Neff, PhD thesis, Friedrich-Alexander-University Erlangen-Nuremberg, **2013**.

[15] C. Markou et al., *PoS* **2023**, *ICRC2023*, 1098.

[16] R. Engel et al., *Computing and Software for Big Science* **2018**, *3*, 2.

[17] C. 8. Collaboration et al. in *Proceedings of 38th International Cosmic Ray Conference — PoS(ICRC2023)*, *Vol. 444*, Conference Name: 38th International Cosmic Ray Conference, SISSA Medialab, **2023**, p. 310.